Two-phase flow of air-water mixture in a minichannel

Fedor Ronshin[1,2], *Karapet* Eloyan[1,*], and *Viacheslav* Cheverda[1,2]

[1] Kutateladze Institute of Thermophysics SB RAS, 630090, Novosibirsk, Russia
[2] Novosibirsk State University, 630090, Novosibirsk, Russia

Abstract. Two-phase systems have a huge potential for solving problems of removing large heat fluxes. To date, mini-channel and microchannel systems are widespread. Of particular interest are the stratified flow regime and the annular flow regime in mini- and micro- channel. It is necessary to know in detail the map of flow regimes for the realization of these flow regimes. In this paper, we present an investigation of flow regimes for a rectangular mini- channel 10 mm wide and 1.1 mm high.

1 Introduction

Two-phase systems in mini and micro channels have received wide application in medicine, microelectronics, power engineering, aircraft and machine building. In medicine, microchannels are used to implement lab-on-chip. In chemistry, chemical reactors are created on the basis of mini and microchannels. In the field of microelectronics, boiling in microchannel is used to cool electronic components; heat exchange in heat exchangers in two-phase systems in mini and micro channels is the basis of the action of heat pipes.

One of the promising ways of removing large heat fluxes from the surface of heat-stressed elements of electronic devices is the use of two-phase flows in microchannels [1,2]. The most efficient flow regimes in the channel (in terms of heat removal) is annular or stratified flow [3]. Flow regimes are of interest for study [4-6], investigation has been carried out for various channel parameters. Of great interest are mini and micro channels with a rectangular cross-section that can be used in cooling systems for microchips. It is important to understand hydrodynamics in such systems to create effective cooling systems. The hydrodynamics of two-phase flow in the minichannels height of 1 mm is investigated in [7]. Regimes in such channels significantly differ from the regimes in microchannels [8].

2 Experimental setup

A schematic diagram of the two-phase mini-channel system is shown in Fig. 1. The system has two working circuits: closed liquid circuit and a gas circuit. The liquid circuit, as seen

* Corresponding author: karapet8883@gmail.com

from Fig. 1, contains pump Grundfos DDE for pumping working liquid. The gas circuit contains a membrane vacuum pump-compressor MVNK 3x4, which produces an output of up to 400 l/min of working gas. To control gas consumption, the Bronkhorst F-111AC-70K flow regulator is used, which has an operating gas flow range from 0 to 100 l/min. Gas and liquid is supplied into the test section, in which a two-phase system is realized. The test section has an inlet for liquid, gas and a common outlet. A rectangular channel with a width of 10 mm and a height of 1.1 mm is constructed. The channel is oriented horizontally. The temperatures of the the substrate, liquid and gas at the inlet are constant and equal to 20 °C. The working fluid is ultrapure water created with the Merck Millipore Direct-Q 3 UV water purification system. In the test section, there is a copper heater, but it is not used in this study.

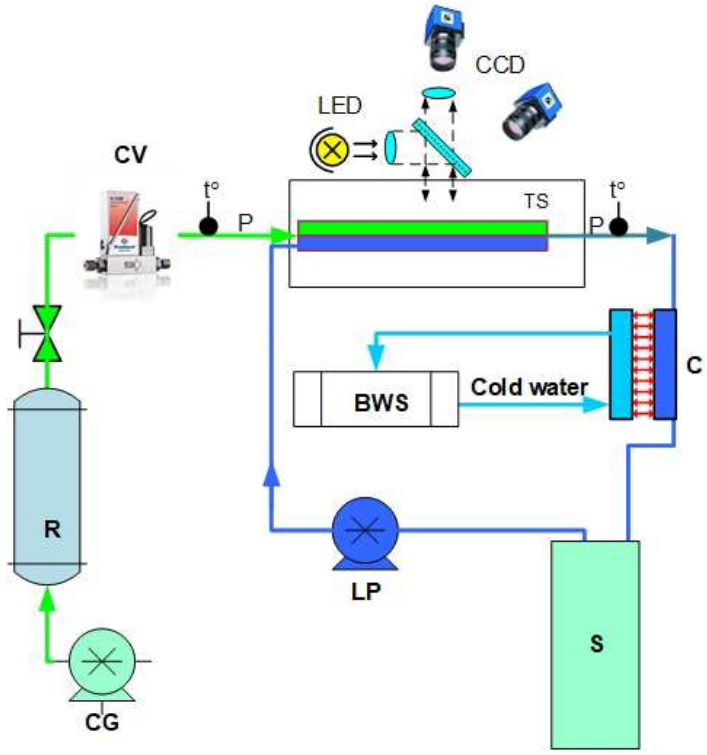

Fig. 1. Schematic of two-phase system: TS – testing section; C – condenser; S – separator; R – receiver; CV – control valve; LP – liquid pump; CG – gas vacuum pump-compressor; BWS – building water supply.

3 Results and discussion

At very low superficial liquid and gas velocities determined as flow rate divided by channel cross-section area) we observed the jet regime. In fig. 2a, we present the image of the jet regime at U_{SL} = 0.102 m/s, U_{SG} = 0.121 m/s. Number 1 denotes the gas entrance and number 2 does liquid nozzle in the figure. The dark square is the heater that we don't use in this experiment. The liquid (3) moves along channel sidewalls and gas jet moves in the central part of the channel. The most part of the bottom channel wall remains dry (4). Is

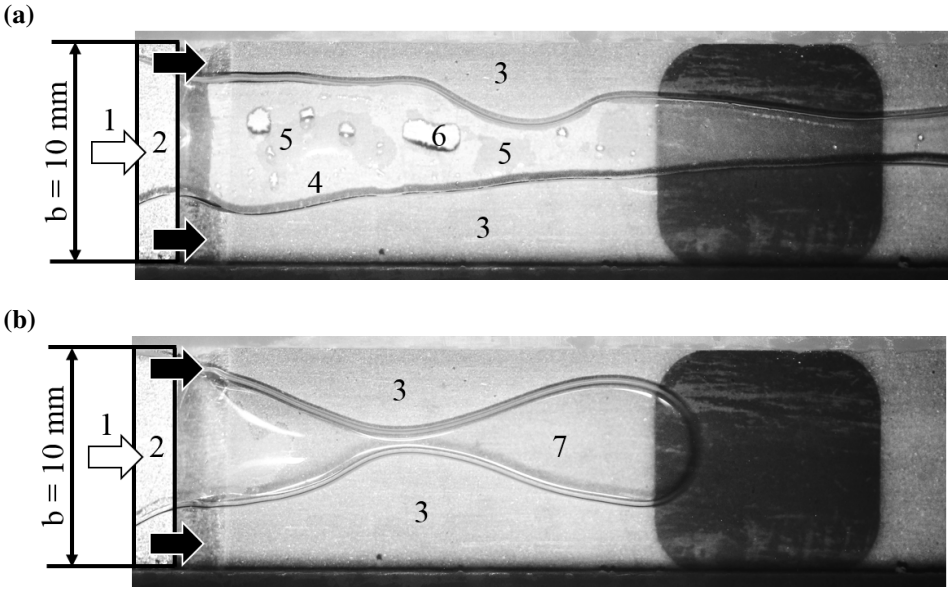

Figure 2. Characteristic photo of the jet flow regime in the channel.

some parts of the bottom channel wall the residual film (5) is observed. The upper channel wall remains dry only sessile droplets (6) are observed. These droplets and residuals film are formed when liquid film is destroyed. The perturbations on the liquid moving along sidewalls are observed. With an increase in superficial liquid velocities the amplitude of perturbation increases. When it becomes equal to the half of channel width the horizontal liquid bridges are formed as a result of interaction of liquid perturbations (fig. 2b), the transition to bubble flow regime occurs. The formation of bubbles from the gas jet is observed (7).

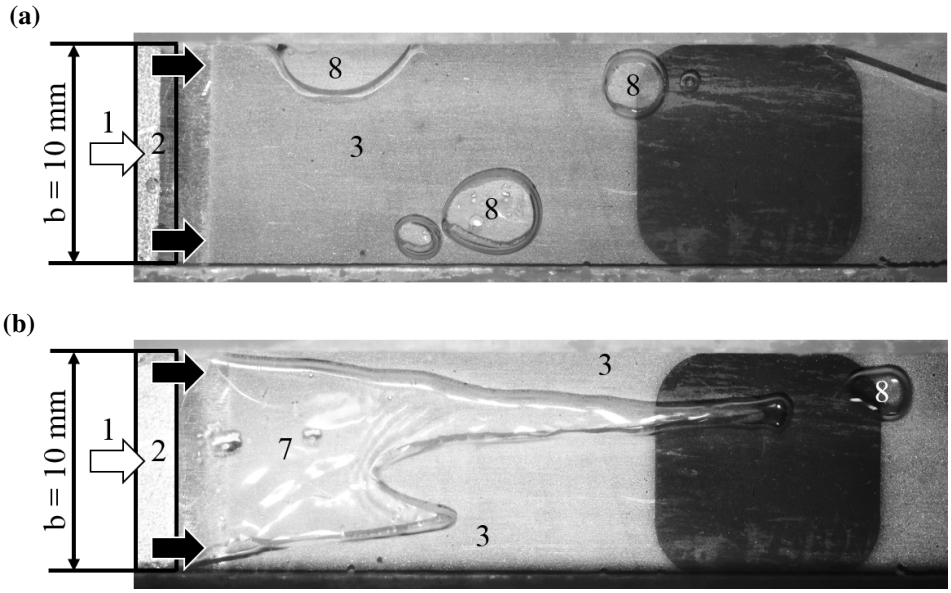

Figure 3. Characteristic photo of the bubble flow regimes in the channel.

In the bubble flow regime, we observe many small bubbles (8). The bubble size and frequency depends on the gas and liquid flow rates. The typical bubble size is about several millimeters and not exceed the channel width. In fig 3a, we present characteristic image of the bubble flow at U_{SL} = 0.17 m/s, U_{SG} = 0.121 m/s. Gas bubbles with different sizes move along the channel. In this case, bubbles are formed directly near the liquid nozzle. With an increase in superficial gas velocity, the frequency of bubble formation increases. Further increasing the superficial gas velocity leads to formation of the gas jet in the inlet section, fig 3b, the transition to the jet regime occurs.

At low superficial liquid velocity (0.02 m/s < U_{SL} < 0.1 m/s) and high superficial gas velocity (U_{SG} > 13 m/s) we observe stratified flow regime. In this regime, a liquid film moves under the action of gas flow. The typical image of stratified flow regime is presented in fig. 3a. The liquid film is denoted in the figure by number 9. In addition, there are impingements on the upper channel wall. With an increase in superficial liquid velocity liquid film on the upper channel wall (10) forms, see fig. 3b. This is the transition to the annular flow regime. In this case, film on the upper channel wall is present only in the initial zone. The differences between films on the upper and bottom channel walls are clearly seen. We don't observe sessile liquid droplets on the upper channel wall when the film on the upper channel wall forms. Further increasing liquid flow rate leads to increase of the area of the film on the upper channel wall, fig 3c.

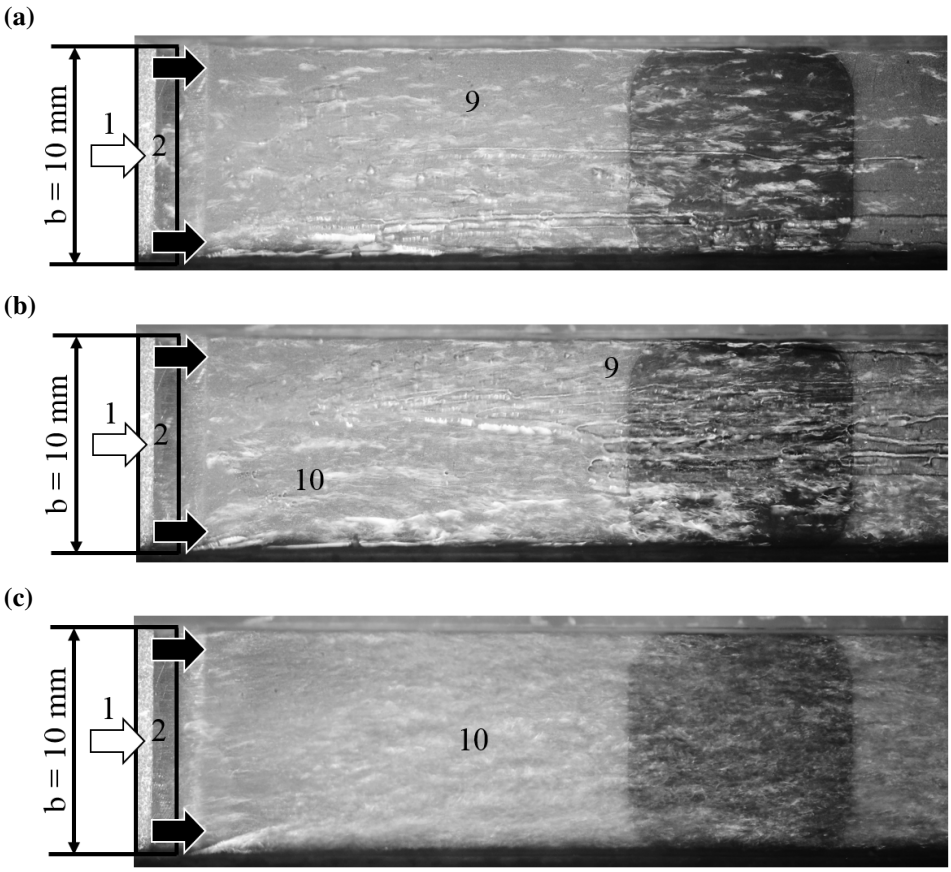

Figure 4. Characteristic photo of the film flow regimes in the channel.

The flow regime map for investigated channel is shown in fig. 4. More than 96 points with different flow rates have been investigated. The following two-phase flow regimes are shown in the regime map: jet (1), bubble (2), stratified (3), and annular (4). The transitions between regimes are investigated.

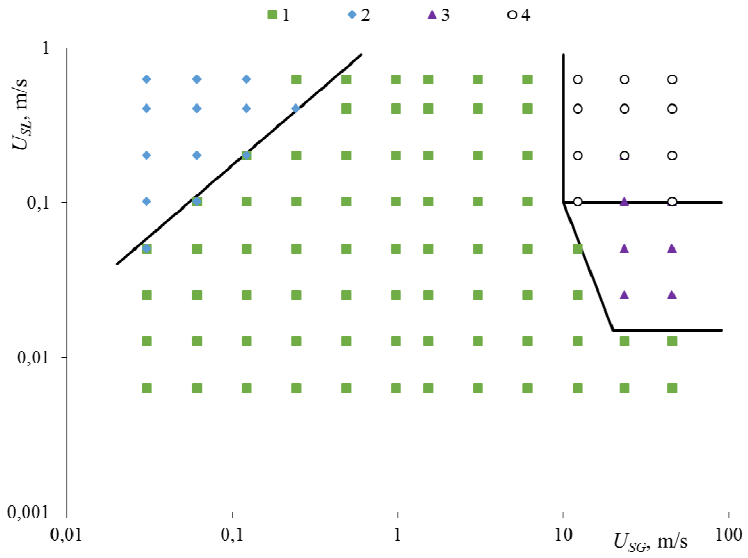

Figure 5. Flow regime map in the channel cross-section of 1.1×10 mm^2.

4 Conclusions

The flow pattern map has been created for wide range of flow parameters (liquid superficial velocity 0.005 – 1 m/s, gas superficial velocity 0.05 – 50 m/s). More than 96 points with different flow rates have been investigated. The four main regimes for minichannel have been identified: jet, bubble, stratified, and annular. In the future this experimental test cell will be used for heat transfer investigations with heating element created by additive technologies. A special structure will be created on the surface in order to intensify heat flux.

The reported study was funded by RFBR according to the research project № 18-48-543034.

References

1. Zhang W., Hibiki T., Mishima K., Mi Y., International Journal of Heat and Mass Transfer, **49**, p. 1058, (2006)
2. Mudawar I., Qu W. International Journal of Heat and Mass Transfer, **47**, p. 2045, (2004)
3. Bar-Cohen A., Holloway C., Journal of Physics: Conference Series, **745**, 022002 (2016)
4. Chinnov E.A., Ron'shin F.V., Kabov O.A., Thermophysics and Aeromechanics, **22**, p. 265, (2015)

5. Rebrov E.V., Theor. Found. Chem. Eng. **44**, p. 355, (2010)
6. Shao N., Gavriilidis A., Angeli P., Chem. Eng. Sci. **64**, p. 2749, (2009)
7. Chinnov E. A., Ron'shin, F. V., Kabov O. A. Thermophysics and Aeromechanics, **22**, p. 621, (2015)
8. Ronshin, F. V., Cheverda V. V., Chinnov E. A., Kabov O. A. Interfacial Phenomena and Heat Transfer, **4**, p. 191, (2016)